Published OnlineFirst July 9, 2019; DOI: 10.1158/2326-6066.CIR-18-0605

Cancer Immunology Miniatures

Cancer Immunology Research

Immunologic Correlates of Pathologic Complete Response to Preoperative Immunotherapy in Hepatocellular Carcinoma

Ahmed Omar Kaseb[1], Luis Vence[2], Jorge Blando[2], Shalini S. Yadav[2], Naruhiko Ikoma[3], Roberto Carmagnani Pestana[4], Jean Nicolas Vauthey[3], James P. Allison[2], and Padmanee Sharma[2]

Abstract

In hepatocellular carcinoma (HCC), surgical resection is associated with high recurrence rate, and no effective adjuvant therapy currently exists. We initiated a pilot randomized trial of perioperative immunotherapy with nivolumab and ipilimumab for resectable HCC. Here, we provide an illustrative report of a case that achieved a complete response and report immunologic correlates of this complete pathologic response to perioperative immunotherapy. Clinical response was correlated with an increase in $CD8^+$ T-cell infiltration, with an increase in two effector T-cell clusters. This study is ongoing, and the final results may contribute to a paradigm shift in the perioperative treatment of HCC, leading to the incorporation of immunotherapy in the curative setting.

Introduction

Hepatocellular carcinoma (HCC) is the most common liver cancer and is the second leading cause of cancer-related death worldwide (1). Surgical resection is potentially curative and has been considered the first-line treatment for operable HCC for the past decade (2). However, the recurrence rates after hepatic resection are high, reaching about 80% at 5 years (3). Preventing relapse after curative treatment remains a significant challenge, and no effective adjuvant therapy has been developed to date (3).

Antibodies blocking the immune-inhibitory pathways PD-1/PD-L1 and CTLA-4 have been used in cancer treatment, including HCC. The antibodies targeting PD-1, pembrolizumab and nivolumab, are currently approved for second-line treatment of HCC, achieving overall response rates of 15% to 20% (4, 5). Anti–CTLA-4, tremelimumab, has shown promising clinical activity in HCC, with response rates of 17% to 26% (6, 7).

The abovementioned results in metastatic HCC compare favorably to FDA-approved treatment options, and this has led to an ongoing, multicenter phase III trial evaluating nivolumab in the adjuvant setting (NCT03383458). A previous preclinical report by Liu and colleagues (8) suggests that efficacy of neoadjuvant immune checkpoint inhibition is increased compared with the same treatment in the adjuvant setting, and feasibility has been demonstrated in non–small cell lung cancer, melanoma, colorectal cancer, and urothelial bladder cancer (9–12). On the basis of these data, we initiated a randomized pilot trial of perioperative immunotherapy for resectable HCC at our institution (ClinicalTrials.gov, NCT03222076). Here, we provide an illustrative report of a case that achieved a complete response and report immunologic correlates of this complete pathologic response to perioperative immunotherapy.

Materials and Methods

Study details

We provide an illustrative case report of a patient that achieved a complete response and report the interim analysis of immune correlates of this complete pathologic response in a randomized phase II trial of perioperative immunotherapy for HCC (NCT03222076) that has accrued 9 patients, with 3 complete responders so far. The clinical trial has three treatment arms: perioperative nivolumab alone at a dose of 3 mg/kg every 2 weeks (arm A) in patients with resectable HCC, perioperative nivolumab (3 mg/kg every 2 weeks) plus ipilimumab (1 mg/kg every 6 weeks; arm B) in patients with resectable HCC, and perioperative nivolumab (3 mg/kg every 2 weeks) plus ipilimumab (1 mg/kg every 6 weeks; arm C) in patients with potentially resectable HCC. All arms included postoperative maintenance immunotherapy for up to 2 years with either single-agent nivolumab or the combination of nivolumab plus ipilimumab at the doses above. The primary endpoint was the safety and tolerability of perioperative therapy, and success was predefined as having at least 13 of 15 subjects receiving their assigned therapy in each arm without grade 3 or higher adverse events, necessitating a delay in the planned surgical resection. Written informed consent was obtained from all patients. The study was conducted in

[1]Department of Gastrointestinal Medical Oncology, The University of Texas MD Anderson Cancer Center, Houston, Texas. [2]Department of Immunology, The University of Texas MD Anderson Cancer Center, Houston, Texas. [3]Department of Surgical Oncology, The University of Texas MD Anderson Cancer Center, Houston, Texas. [4]Department of Cancer Medicine, The University of Texas MD Anderson Cancer Center, Houston, Texas.

Corresponding Authors: Ahmed Omar Kaseb, The University of Texas MD Anderson Cancer Center, Unit 426, 1515 Holcombe Boulevard, Houston, TX 77030. Phone: 713-792-2828; Fax: 713-563-0541; E-mail: akaseb@mdanderson.org; and Padmanee Sharma, padsharma@mdanderson.org

Cancer Immunol Res 2019;7:1390–5

doi: 10.1158/2326-6066.CIR-18-0605

Published OnlineFirst July 9, 2019; DOI: 10.1158/2326-6066.CIR-18-0605

accordance with the Declaration of Helsinki. All bio-specimens collected and used in the study were obtained under an institutional review board–approved protocol (PA13-0291).

Isolation and preparation of peripheral blood mononuclear cells and tissues

Whole blood was collected in cell preparation tubes (CPT) containing sodium heparin (BD Vacutainer) and centrifuged at 800 × *g* for 25 minutes. The interface cells were harvested and washed twice with PBS and centrifuged at 500 × *g* for 10 minutes. Peripheral blood mononuclear cells (PBMC) were then resuspended in AB serum with 10% (vol/vol) DMSO for storage in liquid nitrogen until the assays were performed. The time points collected and analyzed were pretreatment, post-Ipi/Nivo 1 (cycle 2), post-Ipi/Nivo 2 (cycle 3), posttreatment (hepatic resection), and posttreatment (cycle 6). Fresh tumor tissue was dissociated with GentleMACS system (Miltenyi Biotec) as per the manufacturer's instructions, collected, and subsequently prepared for mass cytometry analysis.

Mass cytometry

Mass cytometry (CyTOF) analyses were performed on liver lesions before treatment (pretreatment) and at the time of hepatic resection (posttreatment) to characterize the phenotype and subpopulations of tumor-infiltrating lymphocytes (TIL), and adjacent nontumoral liver tissue, as well as PBMCs. Single-cell suspensions were stained with 36 antibodies [CD45, CD326, TIGIT, CD68, CD73, CD4, CD8a, ICOS (CD278), OX40 (CD134), LAG-3 (CD223), PD-L1 (CD274), CD3, Galectin-9, TIM-3, HVEM (CD270), CD27, CD86, PD-1, VISTA, CD28, CD70, FoxP3, BTLA (CD272), 41BBL (CD137L), KI67, ICOSL (CD275), CD80, B7-H4, B7-H3, CTLA-4 (CD152), GITR (CD357), PD-L2 (CD273), OX40L, CD137 (4-1BB), CD56, HLA-DR, Ir DNA-Intercalator, and cisplatin]. Antibodies were either purchased preconjugated from Fluidigm or purchased purified and conjugated in-house using MaxPar X8 Polymer kits (Fluidigm) according to the manufacturer's instructions. Briefly, samples were stained fresh with cell surface antibodies in PBS containing 5% goat serum and 30% BSA for 30 minutes at 4°C. After viability staining with 5 μmol/L cisplatin (Fluidigm) in PBS containing 30% BSA, samples were washed in PBS containing 30% BSA, fixed, and permeabilized according to manufacturers' instructions using the FoxP3 staining buffer set (eBioscience) before being incubated with intracellular antibodies in permeabilization buffer for 30 minutes at 4°C. Samples were washed and incubated in Ir intercalator (Fluidigm) and stored at 4°C until acquisition, generally within 12 hours. Right before acquisition samples were washed and resuspended in water containing EQ 4 element beads (Fluidigm). Samples were acquired on a Helios mass cytometer (Fluidigm).

Mass cytometry analysis

Files (fcs) were normalized using a bead-based normalization software for mass cytometry data (R package premessa, Parker Institute for Cancer Immunotherapy; ref. 13). Samples were then manually gated in FlowJo by event length, by live/dead discrimination, and for populations of interest using lineage markers (CD45) for separate analyses. Data were then exported into MATLAB as fcs files for downstream analysis and arcsinh transformed using a coefficient of 5 [x_transformed = arsinh(x/5)]. To visualize the high-dimensional data in two dimensions, the t-Distributed Stochastic Neighbor Embedding (t-SNE) dimension reduction algorithm (14, 15) was applied to the cells, using all channels besides those used to manually gate the population of interest (e.g., CD45).

Mass cytometry clustering

Clustering analysis was performed using the MATLAB implementation of the PhenoGraph clustering algorithm (16). Clusters were identified using PhenoGraph on all the samples in the space formed by these principal components, with the parameter k for the number of nearest neighbors selected uniquely for each sample using the formula k = minimum (0.002* number of cells, 10). PhenoGraph was run with parameter k = 30, resulting in 30 clusters in the $CD45^+$ analysis.

IHC staining and analysis

Hematoxylin and eosin (H&E) and IHC staining were performed on formalin-fixed, paraffin-embedded tissue sections. Tissues were fixed in 10% formalin, embedded in paraffin, and transversely sectioned. Four-micron–thick sections were used for the histopathologic study. Sections were stained with mouse or rabbit anti-human mAbs against CD3 (Dako, catalog no. A0452), CD8 (Thermo Fisher Scientific, MS-457-S), CD45RO (Novocastra, PA0146), Gr-B (Leica Microsystems, PA0291), PD-L1 (Cell Signaling Technology, 13684S), and FoxP3 (BioLegend, catalog no. 320102). All sections were counterstained with hematoxylin, and processed with peroxidase-conjugated avidin/biotin and 3′-3-diaminobenzidine (DAB) substrate (Leica Microsystems). Slides were scanned and digitalized using the scanscope system from Scanscope XT, Aperio/Leica Technologies. Quantitative analysis of IHC staining was conducted using the image analysis software ImageScope-Aperio/Leica. Five random areas (1 mm^2 each) comprised of each pretreatment tumoral areas and posttreatment scar inflammatory tissues were selected using a customized algorithm for each marker to determine the number of positive cells at 20× magnification. The data are expressed as a density (total number of positive cells/mm^2 area). IHC staining was interpreted in conjunction with H&E-stained sections.

Case report

A 66-year-old woman with previously treated chronic hepatitis C virus (HCV) infection was diagnosed with localized, resectable, T2N0M0 (stage II), poorly to moderately differentiated HCC. Laboratory examination results demonstrated elevated alpha-fetoprotein (AFP; 681 ng/mL), and a CT scan showed two discrete liver lesions measuring 4.6 × 3.5 cm and 4.5 × 3.1 cm, both in liver segment 3 (Fig. 1A). Hepatitis C viral load was undetectable at time of diagnosis and remained undetectable throughout the treatment. The patient was randomly enrolled in arm B, of preoperative combination nivolumab plus ipilimumab. She was scheduled to receive 240 mg of intravenous nivolumab every 2 weeks for three doses, plus a single dose of 1 mg/kg i.v. ipilimumab on day 1 of the first cycle. However, the third dose of nivolumab was omitted because she experienced a transient grade 3 elevation of transaminases. Aspartase transaminase (AST) and alanine transaminase (ALT) returned to baseline after 8 weeks, and no additional measures were required.

At posttreatment, a preoperative CT scan demonstrated a treatment response: Both lesions were downsized to 3.5 cm in the maximum diameter and had a cyst-like appearance, without

Published OnlineFirst July 9, 2019; DOI: 10.1158/2326-6066.CIR-18-0605

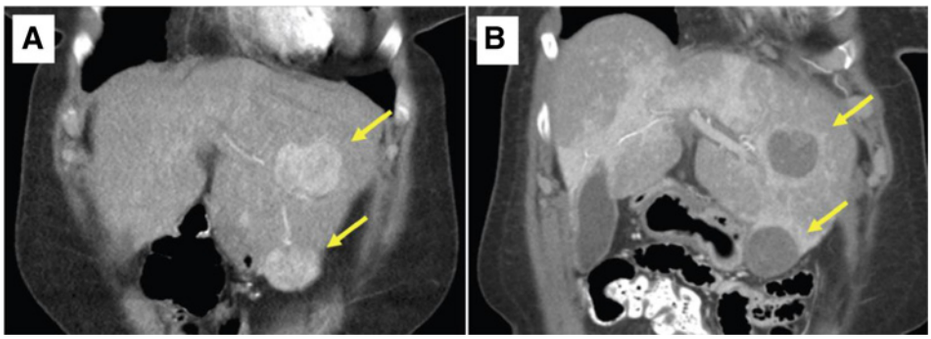

Figure 1.
Pre- and posttreatment CT scans of the responding patient. Arterial phase CT scans taken pretreatment (**A**) and posttreatment (**B**) after one dose of nivolumab plus ipilimumab, followed by one dose of single-agent nivolumab. The tumors initially showed arterial enhancement consistent with HCC but lost this enhancement after treatment.

arterial enhancement (Fig. 1B). AFP also decreased to 25 ng/mL. Four weeks after the second dose of nivolumab, the patient underwent resection of anatomic liver segment 3. The intraoperative liver appearance was normal, with minimal nodularity, and the postoperative course was uncomplicated. Pathologic examination revealed two hemorrhagic and necrotic liver lesions (3.0 and 3.7 cm in diameter), with no viable tumor cells. The patient resumed immunotherapy as per protocol (Fig. 2A) 4 weeks after surgery, with no additional grade 3 or higher toxicity.

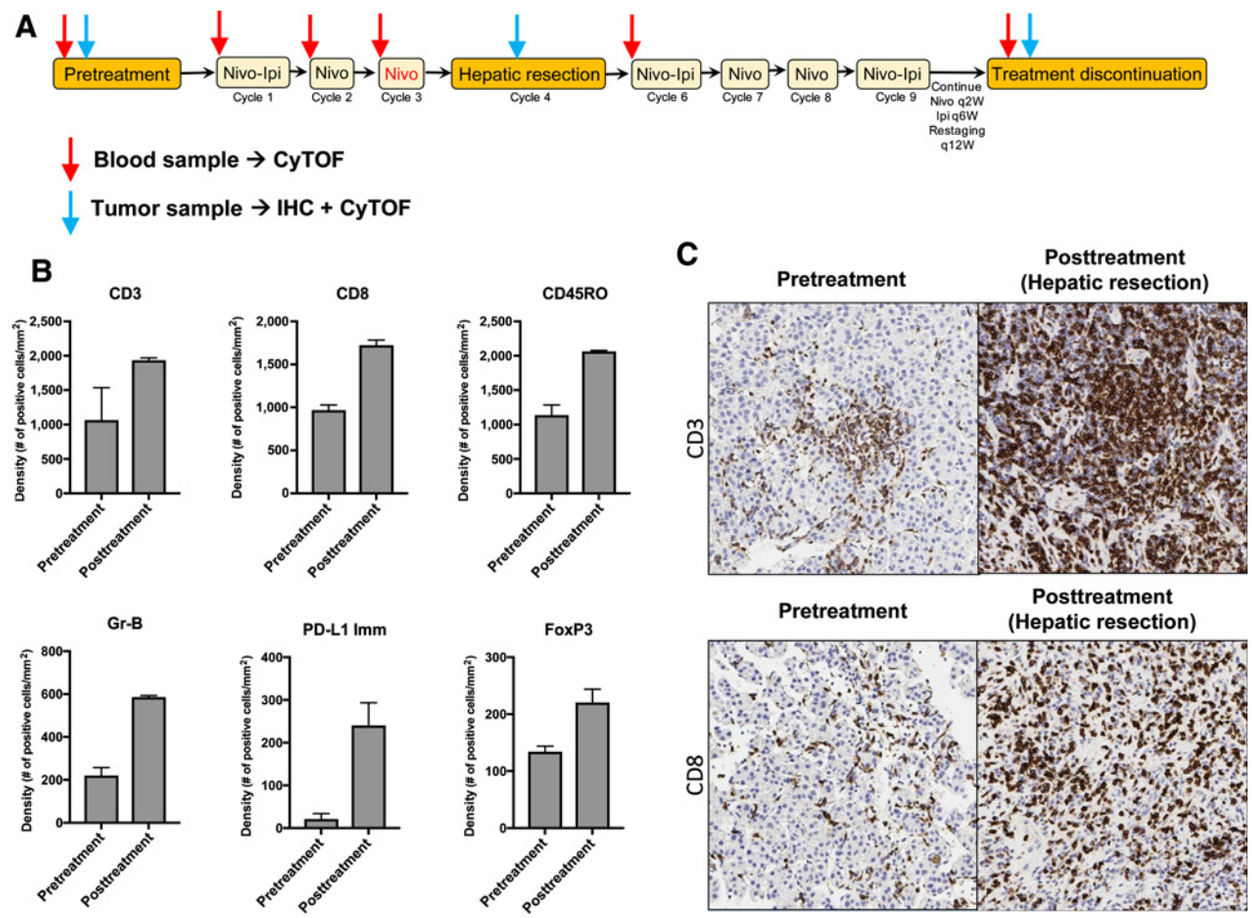

Figure 2.
Clinical trial schema and IHC analysis showing favorable immune infiltration posttreatment in the responder. **A,** Clinical trial NCT03222076 arm A schema indicating when samples were collected. The dose of nivolumab (indicated in red) was not given due to hepatotoxicity. Time points for blood and tumor tissue collection and the assays performed are indicated by red and blue arrows. q2w, every 2 weeks; q6w, every 6 weeks; q12w, every 12 weeks. **B** and **C,** IHC analysis of pre- and posttreatment hepatic tissues from the HCC patient. **B,** IHC analysis of total T cells ($CD3^+$), $CD8^+$ T cells, CD45RO-expressing cells, granzyme B (Gr-B)–expressing cells, FoxP3-expressing cells (regulatory T cells), and PD-L1–expressing immune cells (PD-L1 Imm). Mean density + SD is shown for five different regions in the liver at each timepoint. **C,** Representative IHC images of $CD3^+$ and $CD8^+$ T cells pre- and posttreatment (after resection) from one representative region is shown at a maginification of 20×.

Published OnlineFirst July 9, 2019; DOI: 10.1158/2326-6066.CIR-18-0605

Results

A total of 9 patients have been enrolled at the time of analysis, 5 in arm A and 4 in arm B. There were no delays in surgery related to immunotherapy treatment. Pathologic complete response was observed in 3 of 9 patients (33.3%). The case presented here is the first of these responders.

Immune correlates of complete response

An IHC analysis of the immune infiltrates in the tumor microenvironment showed an increase in T-cell infiltration in posttreatment tissue compared with pretreatment tissue (Fig. 2B and C). The infiltrates were predominantly composed of $CD8^+$ T cells (Fig. 2B and C), and the expression T-cell activation markers CD45RO and granzyme B increased 2- and 3-fold, respectively (Fig. 2B). Foxp3 and PD-L1 expression on immune cells was increased after treatment (Fig. 2B).

CyTOF analysis of the leukocytes from tumor, normal liver tissue, and PBMCs from pretreatment and posttreatment tissue yielded 30 clusters among the different leukocyte subpopulations (Fig. 3A). These clusters expressed different markers on the surface and intracellularly as shown in the heatmap in Fig 3B. The analysis of these clusters showed an increase in two effector $CD8^+$ T-cell clusters in the posttreatment tumor tissue (Fig. 3C and D). These clusters consisted of $CD3^+CD8^+CD45RO^+Eomes^+$ cells (cluster 5) and $CD3^+CD8^+CD45RO^+Eomes^+CD57^+CD38^{low}$ cells (cluster 12; Fig. 3C and D, respectively). Regulatory T cells (Treg; $CD3^+CD4^+CD45RO^+Foxp3^+ICOS^+$ cells, cluster 8) also showed an increase in posttreatment tumor tissue (Fig. 3E). The increase of these three clusters was in concordance with the increase in $CD3^+$, $CD8^+$, $CD45RO^+$, and $Foxp3^+$ T cells seen with IHC analysis (Fig. 2B). Subsequently, we evaluated the $CD8^+$ T-cell/Treg ratio, which was calculated using the ratio of clusters 5 and 12 over cluster 8. The $CD8^+$ T-cell/Treg ratio in the tumor microenvironment increased slightly after treatment with nivolumab and ipilimumab, from 4.7 to 6.2 (Fig. 3F). This ratio did not change in adjacent nontumoral liver samples (0.6–0.4; Fig. 3F).

Discussion

We provide a report of immunologic correlates of a complete pathologic response to preoperative immune checkpoint inhibitors in HCC. Surgical resection was performed safely, with no delays or complications. The clinical response was correlated with an increase in $CD8^+$ T-cell infiltration, with an 11-fold increase in $CD3^+CD8^+CD45RO^+Eomes^+$ and a 6-fold increase in $CD3^+CD8^+CD45RO^+Eomes^+CD57^+CD38^{low}$ clusters. The clusters that increased after treatment were effector $CD8^+$ T cells

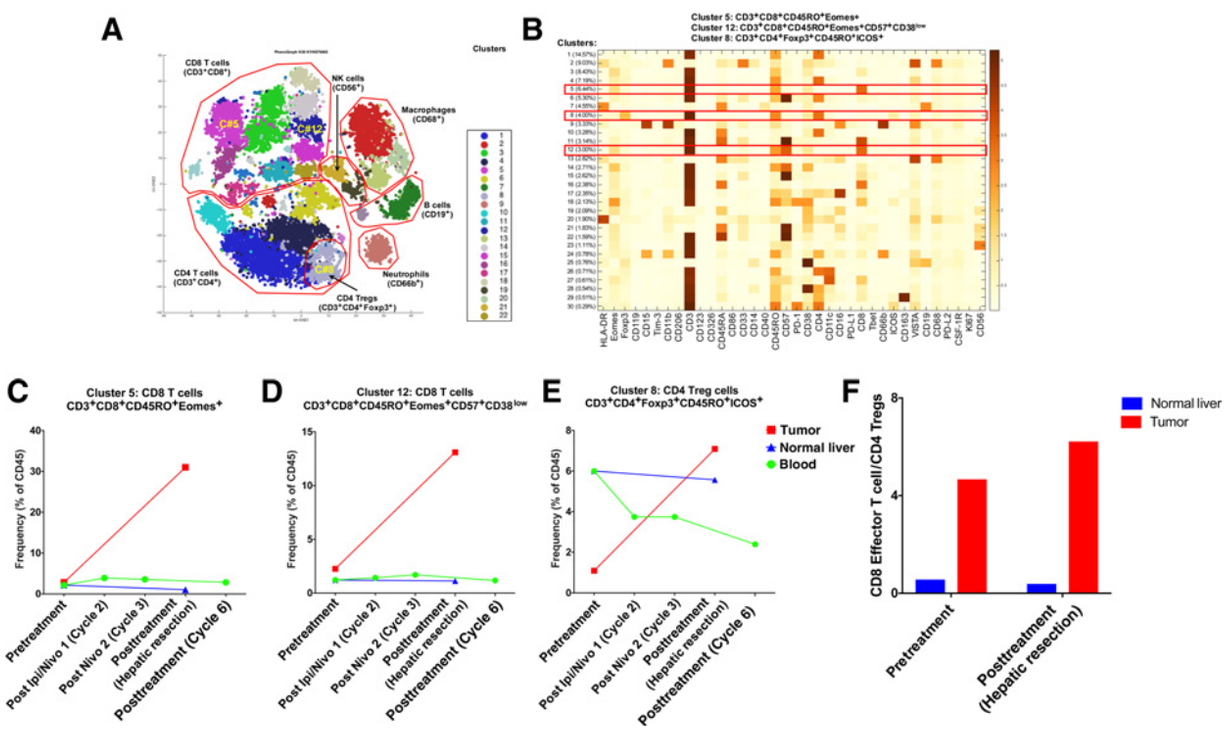

Figure 3.

Mass cytometry (CyTOF) analysis of tissues and blood from the responder. Phenograph analysis was performed to determine the frequencies of each cluster in the total $CD45^+$ population. **A,** tSNE plot showing the different clusters identified within each cell subpopulation. Clusters 5, 12 ($CD8^+$ T-cell effectors), and 8 (regulatory T cell) are shown. NK, natural killer. **B,** Heatmap showing marker expression and frequencies of the different clusters identified. Clusters 5, 12, and 8 are marked by red boxes. **C,** Frequency of activated $CD8^+$ T cells (cluster 5) for pre- and posttreatment tumor tissue, pre- and posttreatment nontumoral liver (normal liver), and pre- and posttreatment PBMCs at various time points as indicated. **D,** Frequency of activated $CD8^+$ T cells (cluster 12) for pre- and posttreatment tissue, pre- and posttreatment nontumoral liver, and pre- and posttreatment PBMCs at various time points as indicated. **E,** Frequency of $CD4^+$ Tregs (cluster 8) for pre- and posttreatment tissue, pre- and posttreatment nontumoral liver, and pre- and posttreatment PBMCs at various time points as indicated. **F,** Effector $CD8^+$ T-cell/Treg ratio pre- and posttreatment in tumors and nontumoral liver samples.

Published OnlineFirst July 9, 2019; DOI: 10.1158/2326-6066.CIR-18-0605

expressing CD45RO and Eomes, both of which are very important for their antitumor function (17, 18). CD57 expressed by cells in cluster 12 defines a $CD8^+$ T-cell subpopulation with high cytotoxic activity (19). Taken together, these data support the notion of highly cytotoxic effector $CD8^+$ T cells entering the tumor after preoperative combined checkpoint inhibitor treatment, where they can then mount antitumor responses against HCC. T-cell infiltration was present in the tumor microenvironment prior to treatment, and this could have been due, at least in part, to prior chronic HCV infection (20), even if viral loads were not detectable at the time of treatment.

We observed an upregulation of cytotoxic and effector memory cell markers in our patient after preoperative treatment with nivolumab/ipilimumab, detected both by IHC analysis (CD3, CD8, CD45RO, and granzyme B) and CyTOF (CD3, CD8, and CD45RO). Similarly, it has been reported that an immunoscore that characterizes cytotoxic and effector memory cells can be correlated with response and outcomes in colorectal cancer (21). Our analysis showed increased PD-L1 expression following neoadjuvant immunotherapy with nivolumab plus ipilimumab. We hypothesize that an increase in $CD8^+$ T-cell frequency in the tumor after treatment leads to T-cell activation, PD-1 expression, and IFNγ production within the tumor microenvironment, which in turn may also induce PD-L1 expression (22, 23). A potential additive or synergistic effect of the nivolumab/ipilimumab combination treatment has been described in melanoma (24). These findings support our observation that the patient in our study experienced a complete response.

We demonstrated that the cluster of $CD3^+CD4^+CD45RO^+Foxp3^+ICOS^+$ cells selectively increased in the tumor microenvironment after preoperative immunotherapy. Interestingly, the presence of $CD4^+Foxp3^+$ Tregs, especially $ICOS^+Foxp3^+$ Tregs, has been generally linked to poor prognosis and decreased survival in HCC as a result of the suppression of antitumor responses (25). However, accumulating data suggest that $Foxp3^+$ T cells in human cancer are heterogeneous in phenotype and function (26). In human colorectal cancer and breast cancer, for example, the presence of $Foxp3^+$ Tregs has been reported to be predictive of favorable outcome (27, 28). In our case, both Tregs and $CD8^+$ effector T cells increased simultaneously. This increase may be an indicator of a $CD8^+$ T-cell response, which might overcome the immunosuppressive effects of Tregs. Indeed, the $CD8^+$ T-cell/Treg ratio increased slightly in the tumor microenvironment after treatment with nivolumab and ipilimumab, whereas this ratio did not change in adjacent nontumoral liver samples. Previous reports have proposed the relevance of the intratumoral balance of regulatory and cytotoxic T cells in HCC (25). A previous analysis of 302 patients demonstrates that a high intratumoral $CD8^+$ effector T-cell/Treg ratio is significantly associated with an improved prognosis following hepatic resection (25). Patients with high $CD8^+$ effector T-cell/Treg ratios have significantly longer overall survival (86 months) and disease-free survival (105 months) than those with low $CD8^+$ T-cell/Treg ratios (31 and 23 months, respectively; ref. 29).

This study is ongoing, with an expected total enrollment of 45 patients, and we will perform immune monitoring on biological samples from all patients enrolled. The final results may provide more insight into our initial findings reported here and may contribute to a paradigm shift in perioperative immunotherapy for HCC. This, in turn, may lead to a decreased incidence of HCC recurrence and improved HCC outcomes through the incorporation of immunotherapy in the curative setting.

Disclosure of Potential Conflicts of Interest

P. Sharma has ownership interest (including stock, patents, etc.) in Jounce, Neon, Constellation, Forty Seven, and is a consultant/advisory board member for Jounce, Neon, Marker, Pieris, Imaginab, Constellation, Forty Seven, Optera, Hummingbird, BioAtla, Codiak, Polaris, and Oncolytics. No potential conflicts of interest were disclosed by the other authors.

Authors' Contributions

Conception and design: A.O. Kaseb, N. Ikoma, R.C. Pestana, P. Sharma
Development of methodology: A.O. Kaseb, P. Sharma
Acquisition of data (provided animals, acquired and managed patients, provided facilities, etc.): A.O. Kaseb, L. Vence, N. Ikoma, P. Sharma
Analysis and interpretation of data (e.g., statistical analysis, biostatistics, computational analysis): A.O. Kaseb, L. Vence, J. Blando, S.S. Yadav, J.N. Vauthey, J.P. Allison, P. Sharma
Writing, review, and/or revision of the manuscript: A.O. Kaseb, L. Vence, J. Blando, S.S. Yadav, N. Ikoma, R.C. Pestana, J.N. Vauthey, J.P. Allison, P. Sharma
Administrative, technical, or material support (i.e., reporting or organizing data, constructing databases): A.O. Kaseb, R.C. Pestana
Study supervision: A.O. Kaseb, J.N. Vauthey, J.P. Allison

Acknowledgments

This work was funded by Bristol-Myers Squibb.

Received August 31, 2018; revised February 4, 2019; accepted July 2, 2019; published first July 9, 2019.

References

1. Torre LA, Bray F, Siegel RL, Ferlay J, Lortet-Tieulent J, Jemal A. Global cancer statistics, 2012. CA Cancer J Clin 2015;65:87–108.
2. Pang TC, Lam VW. Surgical management of hepatocellular carcinoma. World J Hepatol 2015;7:245–52.
3. Bruix J, Takayama T, Mazzaferro V, Chau G-Y, Yang J, Kudo M, et al. Adjuvant sorafenib for hepatocellular carcinoma after resection or ablation (STORM): a phase 3, randomised, double-blind, placebo-controlled trial. Lancet Oncol 2015;16:1344–54.
4. Zhu AX, Finn RS, Edeline J, Cattan S, Ogasawara S, Palmer D, et al. Pembrolizumab in patients with advanced hepatocellular carcinoma previously treated with sorafenib (KEYNOTE-224): a non-randomised, open-label phase 2 trial. Lancet Oncol 2018;19:940–52.
5. El-Khoueiry AB, Sangro B, Yau T, Crocenzi TS, Kudo M, Hsu C, et al. Nivolumab in patients with advanced hepatocellular carcinoma (CheckMate 040): an open-label, non-comparative, phase 1/2 dose escalation and expansion trial. Lancet North Am Ed 2017;389:2492–502.
6. Duffy AG, Ulahannan SV, Makorova-Rusher O, Rahma O, Wedemeyer H, Pratt D, et al. Tremelimumab in combination with ablation in patients with advanced hepatocellular carcinoma. J Hepatol 2017;66:545–51.
7. Sangro B, Gomez-Martin C, de la Mata M, Iñarrairaegui M, Garralda E, Barrera P, et al. A clinical trial of CTLA-4 blockade with tremelimumab in patients with hepatocellular carcinoma and chronic hepatitis C. J Hepatol 2013;59:81–8.
8. Liu J, Blake SJ, Yong MCR, Harjunpää H, Ngiow SF, Takeda K, et al. Improved efficacy of neoadjuvant compared to adjuvant immunotherapy to eradicate metastatic disease. Cancer Discov 2016;6:1382–99.
9. Amaria RN, Reddy SM, Tawbi HA, Davies MA, Ross MI, Glitza IC, et al. Neoadjuvant immune checkpoint blockade in high-risk resectable melanoma. Nat Med 2018;24:1649–54.
10. Forde PM, Chaft JE, Smith KN, Anagnostou V, Cottrell TR, Hellmann MD, et al. Neoadjuvant PD-1 blockade in resectable lung cancer. N Engl J Med 2018;378:1976–86.

Published OnlineFirst July 9, 2019; DOI: 10.1158/2326-6066.CIR-18-0605

11. Necchi A, Anichini A, Raggi D, Briganti A, Massa S, Lucianò R, et al. Pembrolizumab as neoadjuvant therapy before radical cystectomy in patients with muscle-invasive urothelial bladder carcinoma (PURE-01): an open-label, single-arm, phase II study. J Clin Oncol 2018;36:3353–60.
12. Chalabi M, Fanchi LF, Van den Berg JG, Beets GL, Lopez-Yurda M, Aalbers AG, et al. LBA37_PRNeoadjuvant ipilimumab plus nivolumab in early stage colon cancer. Ann Oncol 2018;29(suppl_8):mdy424.047.
13. Finck R, Simonds EF, Jager A, Krishnaswamy S, Sachs K, Fantl W, et al. Normalization of mass cytometry data with bead standards. Cytometry A 2013;83:483–94.
14. Amir el AD, Davis KL, Tadmor MD, Simonds EF, Levine JH, Bendall SC, et al. viSNE enables visualization of high dimensional single-cell data and reveals phenotypic heterogeneity of leukemia. Nat Biotechnol 2013;31:545–52.
15. van der Maaten LH. Visualizing data using t-SNE. J Mach Learn Res 2008;9: 2579–605.
16. Levine JH, Simonds EF, Bendall SC, Davis KL, Amir el AD, Tadmor MD, et al. Data-driven phenotypic dissection of AML reveals progenitor-like cells that correlate with prognosis. Cell 2015;162:184–97.
17. Li G, Yang Q, Zhu Y, Wang H-R, Chen X, Zhang X, et al. T-Bet and Eomes regulate the balance between the effector/central memory T cells versus memory stem like T cells. PLoS One 2013;8:e67401.
18. Zhu Y, Ju S, Chen E, Dai S, Li C, Morel P, et al. T-bet and eomesodermin are required for T cell-mediated antitumor immune responses. J Immunol 2010;185:3174–83.
19. Wu RC, Hwu P, Radvanyi LG. New insights on the role of CD8(+)CD57(+) T-cells in cancer. Oncoimmunology 2012;1:954–6.
20. Ramzan M, Sturm N, Decaens T, Bioulac-Sage P, Bancel B, Merle P, et al. Liver-infiltrating CD8+ lymphocytes as prognostic factor for tumour recurrence in hepatitis C virus-related hepatocellular carcinoma. Liver Int 2015;36:434–44.
21. Galon J, Costes A, Sanchez-Cabo F, Kirilovsky A, Mlecnik B, Lagorce-Pagès C, et al. Type, density, and location of immune cells within human colorectal tumors predict clinical outcome. Science 2006;313:1960–4.
22. Huang RR, Jalil J, Economou JS, Chmielowski B, Koya RC, Mok S, et al. CTLA4 blockade induces frequent tumor infiltration by activated lymphocytes regardless of clinical responses in humans. Clin Cancer Res 2011;17: 4101–9.
23. Mandai M, Hamanishi J, Abiko K, Matsumura N, Baba T, Konishi I. Dual faces of IFN-γ in cancer progression: a role of PD-L1 induction in the determination of pro- and anti-tumor immunity. Clin Cancer Res 2016;22: 2329–34.
24. Carlino MS, Long GV. Ipilimumab combined with nivolumab: a standard of care for the treatment of advanced melanoma? Clin Cancer Res 2016;22: 3992–8.
25. Tu J-F, Ding Y-H, Ying X-H, Wu F-Z, Zhou X-M, Zhang D-K, et al. Regulatory T cells, especially ICOS(+) FOXP3(+) regulatory T cells, are increased in the hepatocellular carcinoma microenvironment and predict reduced survival. Sci Rep 2016;6:35056.
26. Tanaka A, Sakaguchi S. Regulatory T cells in cancer immunotherapy. Cell Res 2017;27:109–18.
27. Ladoire S, Martin F, Ghiringhelli F. Prognostic role of FOXP3+ regulatory T cells infiltrating human carcinomas: the paradox of colorectal cancer. Cancer Immunol Immunother 2011;60:909–18.
28. Salama P, Phillips M, Grieu F, Morris M, Zeps N, Joseph D, et al. Tumor-infiltrating FOXP3+ T regulatory cells show strong prognostic significance in colorectal cancer. J Clin Oncol 2009;27:186–92.
29. Gao Q, Qiu S-J, Fan J, Zhou J, Wang X-Y, Xiao Y-S, et al. Intratumoral balance of regulatory and cytotoxic T cells is associated with prognosis of hepatocellular carcinoma after resection. J Clin Oncol 2007;25: 2586–93.

Published OnlineFirst July 9, 2019; DOI: 10.1158/2326-6066.CIR-18-0605

Cancer Immunology Research

Immunologic Correlates of Pathologic Complete Response to Preoperative Immunotherapy in Hepatocellular Carcinoma

Ahmed Omar Kaseb, Luis Vence, Jorge Blando, et al.

Cancer Immunol Res 2019;7:1390-1395. Published OnlineFirst July 9, 2019.